

expressing the Parkinson's disease-associated UCH-L1 I93M mutant. *Neurochem. Int.* 50 (2007) 119-129

Nishimoto, M., Furuta, A., Aoki, S., Kudo, Y., Miyakawa, H. and Wada, K.: PACAP/PAC1 autocrine system promotes proliferation and astrogenesis in neural progenitor cells. *Glia* 55 (2007) 317-327

Ohashi, H., Nishikawa, K., Ayukawa, K., Hara, Y., Nishimoto, M., Kudo, Y., Abe, T., Aoki, S. and Wada, K.: Alpha 1-adrenoceptor agonists protect against stress-induced death of neural progenitor cells. *Eur. J. Pharmacol.* 573 (2007) 20-28

## 2. 学会発表

(国際学会)

Wada, K., Yamauchi, R., Sakurai, M., Furuta, A., Wada, E., Sekiguchi, M. and Aoki, S.: Novel therapeutic targets in glia-neuron interaction: G-Protein coupled receptors and deubiquitinating enzymes. International Society for Neurochemistry jointly with the European Society for Neurochemistry. 20<sup>th</sup> Biennial Meeting, 8.22, 2005

Aoki, S., Sun, Y., Nishikawa, K., Yuda, H., Osaka, H., Wang, Y., Fukazawa, N. and Wada, K.: Solo/trio8, A Membrane-associated Short Isoform of Trio, Modulates Endosome Dynamics and Neurite Elongation, ASCB 45th annual meeting, San Diego, CA, 12.11, 2006

大橋洋輝、君和田友美、西川香里、青木俊介、和田圭司: 成熟個体脳由来の神経系前駆細胞における G 蛋白質共役型受容体の発現解析. 第 28 回日本分子生物学会年会、福岡、12. 9, 2005

北村悠輔、君和田友美、松本 隆、和田圭司: 交換モンテカルロ法を用いた遺伝子制御ネットワーク推定による核内受容体ネットワークの解析. 日本バイオインフォマティクス学会、第 10 回システムバイオロジー研究会、3. 30, 2006

君和田友美、桜井省花子、大橋洋輝、青木俊介、

富永悌二、和田圭司: 培養神経幹/前駆細胞の神経分化における時計遺伝子の関与. 第 30 回日本神経科学大会・第 50 回日本神経化学学会大会・第 17 回日本神経回路学会大会・合同大会、横浜、9. 11, 2007

H. 知的所有権の出願・登録状況

1. 特許取得  
特になし

2. 実用新案登録  
特になし

3. その他  
特になし

## Ⅱ. 研究成果の刊行に関する一覧表

研究成果の刊行に関する一覧表

所属施設 国立精神・神経センター

氏名 高坂 新一

雑誌

発表者氏名	論文タイトル名	発表誌名	巻号	ページ	出版年
Kamitori, K., Tanaka, M., Okuno-Hirasawa, T., <u>Kohsaka, S.</u>	Receptor related to tyrosine kinase RYK regulates cell migration during cortical development.	Biochem. Biophys. Res. Commun.	330	446-453	2005
Hirasawa, T., Ohsawa, K., Imai, Y., Ondo, Y., Akazawa, C., Uchino, S., <u>Kohsaka, S.</u>	Visualization of microglia in living tissues by using Iba1-EGFP transgenic mice.	J. Neurosci. Res.	81	357-362	2005
Yogosawa, S., Hatakeyama, S., Nakayama, K I., Miyoshi, H., <u>Kohsaka, S.</u> , Akazawa, C.	Ubiquitylation and degradation of serum-inducible kinase by hVPS18, a RING-H2 type ubiquitin ligase.	J. Biol. Chem.	280	41619-41627	2005
Hattori, K., Uchino, S., Isosaka, T., Mackawa, M., Iyo, M., Sato, T., <u>Kohsaka, S.</u> , Yagi, T., <u>Yuasa, S.</u>	Fyn is required for haloperidol-induced catalepsy in mice.	J. Biol. Chem.	281	7129-7135	2006
Uchino, S., Wada, H., Honda, S., Nakamura, Y., Ondo, Y., Uchiyama, T., Tsutsumi, M., Hirasawa, T., <u>Kohsaka, S.</u>	Direct interaction of PDZ domain-containing synaptic molecule Shank3 with GluR1 AMPA receptor.	J. Neurochem.	97	1203-1214	2006
Ohsawa, K., Irino, Y. Nakamura, Y., Akazawa, C., Inoue, K., <u>Kohsaka, S.</u>	Involvement of P2X4 and P2Y12 receptors in ATP-induced microglia chemotaxis.	Glia	55	604-616	2007
Yamakawa, H., Oyama, S., Mitsuhashi, H., Sasagawa, N., Uchino, S., <u>Kohsaka, S.</u> , Ishiura, S.	Neuroligins 3 and 4X interact with syntrophin-γ2, and the interactions are affected by autism-related mutations.	Biochem. Biophys. Res. Commun.	355	41-46	2007

<p>Koizumi, S., Shigemoto-Mogami, Y., Nasu-Tada, K., Shinozaki, Y., Ohsawa, K., Tsuda, M., Joshi, BV., Jacobson, KA., <u>Kohsaka, S.</u>, Inoue, K.</p>	<p>UDP acting at P2Y6 receptors is a mediator of microglial phagocytosis.</p>	<p>Nature</p>	<p>446</p>	<p>1091-1095</p>	<p>2007</p>
<p>Okamoto, N., Kubota, T., Nakamura, Y., Murakami, R., Nishikubo, T., Tanaka, I., Takahashi, Y., Hayashi, S., Imoto, I., Inazawa, J., Hosokai, N., <u>Kohsaka, S.</u>, Uchino, S.</p>	<p>22q13 microduplication in two patients with common clinical manifestations: A recognizable syndrome?</p>	<p>Am. J. Med. Genet. A.</p>	<p>143A</p>	<p>2804-2809</p>	<p>2007</p>
<p>Irino, Y., Nakamura, Y., Inoue, K., <u>Kohsaka, S.</u>, Ohsawa, K.</p>	<p>Akt activation is involved in P2Y12 receptor-mediated chemotaxis of microglia.</p>	<p>J. Neurosci. Res.</p>		<p>in press</p>	<p>2008</p>

研究成果の刊行に関する一覧表

所属施設 国立精神・神経センター

氏 名 湯浅 茂樹

雑誌

発表者氏名	論文タイトル名	発表誌名	巻号	ページ	出版年
Maekawa, M., Takashima, N., Arai, Y., Nomura, T., Inokuchi, K., <u>Yuasa, S.</u> , Osumi, N.	Pax6 is required for production and maintenance of progenitor cells in postnatal hippocampal neurogenesis.	Genes to Cells	10	1001-1014	2005
Nakahira, E., <u>Yuasa, S.</u>	Neuronal generation, migration and differentiation in the mouse hippocampal primordium as revealed by in utero electroporation.	J. Comp. Neurol.	483	329-340	2005
Kai, N., Iwase, K., Imai, K., Nakahira, E., Soma, M., Ohtsuka, S., Yagi, T., Kobayashi, K., Koga, H., Takiguchi, M., <u>Yuasa, S.</u>	Altered gene expression in the subdivisions of the amygdala of Fyn-deficient mice as revealed by laser capture microdissection and mKIAA cDNA array analysis.	Brain Res.	1073	60-70	2006
Morone, N., Fujiwara, T., Murase, K., Kasai, R.S., Ike, H., <u>Yuasa, S.</u> , Usukura, J., Kusumi, A.	Three-dimensional reconstruction of the membrane skeleton at the plasma membrane interface by electron tomography.	J. Cell Biol.	174	851-862	2006
Zhang, H., Muramatsu, T., Murase, A., <u>Yuasa, S.</u> , Uchimura, K., Kadomatsu, K.	N-Acetylglucosamine 6-O-sulfotransferase-1 is required for brain keratan sulfate biosynthesis and glial scar formation after brain injury.	Glycobiology	16	702-710	2006
Kudo, T., Fujii, T., Ikegami, S., Inokuchi, K., Takayama, Y., Ikehara, Y., Nishihara, S., Togayachi, A., Takahashi, S., Tachibana, K., <u>Yuasa, S.</u> , Narimatsu, H.	Mice lacking $\alpha 1$ , 3-fucosyltransferase IX demonstrate disappearance of Lewis X structure in brain and increased anxiety-like behaviors.	Glycobiology	17	1-9	2007

Ikeshima-Kataoka, H., Saito, S., <u>Yuasa, S.</u>	Tenascin-C is required for proliferation of astrocytes in primary culture.	IN VIVO	21	629-633	2007
Yao, I., Takagi, H., Ageta, H., Kahyo, T., Sato, S., Hatanaka, K., Fukuda, Y., Chiba, T., Morone, N., <u>Yuasa, S.</u> , Inokuchi, K., Ohtsuka, T., Macgregor, GR., Tanaka, K., Setou, M.	Scrapper-dependent ubiquitination of active zone protein RIM1 regulates synaptic vesicle release.	Cell	130	943-957	2007
Mimura, N., <u>Yuasa, S.</u> , Soma, M., Jin, H., Kimura, K., Goto, S., Koseki, H. and Aoe, T.	Altered quality control in the endoplasmic reticulum causes cortical dysplasia in knock-in mice expressing a mutant BiP.	Mol. Cell. Biol.	28	293-301	2008

研究成果の刊行に関する一覧表

所属施設 国立精神・神経センター

氏名 和田 圭司

雑誌

発表者氏名	論文タイトル名	発表誌名	巻号	ページ	出版年
Sakurai, M., Ayukawa, K., Setsuie, R., Nishikawa, K., Hara, Y., Ohashi, H., Nishimoto, M., Abe, T., Kudo, Y., Sekiguchi, M., Sato, Y, Aoki, S., <u>Wada, K.</u>	Ubiquitin C-terminal hydrolase L1 regulates the morphology of neural progenitor cells and modulates their differentiation.	J. Cell Sci.	119	162-171	2006
Fukazawa, N., Ayukawa, K., Nishikawa, K., Ohashi, H., Ichihara, N., Hikawa, Y., Abe, T., Kudo, Y., Kiyama, H., <u>Wada, K.</u> , Aoki, S.	Identification and functional characterization of mouse TPO1 as a myelin membrane protein.	Brain Res.	1070	1-14	2006
Sun, Y. J., Nishikawa, K., Yuda, H., Wang, Y. L., Osaka, H., Fukazawa, N., Naito, A., Kudo, Y., <u>Wada, K.</u> , Aoki, S.	Solo/Trio8, a membrane-associated short isoform of Trio, modulates endosome dynamics and neurite elongation.	Mol. Cell. Biol.	26	6923-6935	2006
Tomita, S., Sekiguchi, M., <u>Wada, K.</u> , Nicoll, R.A., Bredt, D.S.	Stargazin controls the pharmacology of AMPA receptor potentiators.	Proc. Natl. Acad. Sci. U. S. A.	103	10064-10067	2006
Setsuie, R., Wang, Y.L., Mochizuki, H., Osaka, H., Hayakawa, H., Ichihara, N., Li, H., Furuta, A., Sano, Y., Sun, Y.J., Kwon, J., Kabuta, T., Yoshimi, K., Aoki, S., Mizuno, Y., Noda, M., <u>Wada, K.</u>	Dopaminergic neuronal loss in transgenic mice expressing the Parkinson's disease-associated UCH-L1 I93M mutant.	Neurochem. Int.	50	119-129	2007
Nishimoto, M., Furuta, A., Aoki, S., Kudo, Y., Miyakawa, H., <u>Wada, K.</u>	PACAP/PAC1 autocrine system promotes proliferation and astrogenesis in neural progenitor cells.	Glia	55	317-327	2007
Ohashi, H., Nishikawa, K., Ayukawa, K., Hara, Y., Nishimoto, M., Kudo, Y., Abe, T., Aoki, S., <u>Wada, K.</u>	Alpha 1-adrenoceptor agonists protect against stress-induced death of neural progenitor cells.	Eur. J. Pharmacol.	573	20-28	2007

### Ⅲ. 研究成果の刊行物・別刷



# Visualization of Microglia in Living Tissues Using Iba1-EGFP Transgenic Mice

T. Hirasawa, K. Ohsawa, Y. Imai, Y. Ondo, C. Akazawa, S. Uchino, and S. Kohsaka\*

Department of Neurochemistry, National Institute of Neuroscience, Kodaira, Tokyo, Japan

Microglia are thought to play important roles not only in repairing injured tissue but in regulating neuronal activity, and visualizing the cells is very useful as a means of further investigating the function of microglia *in vivo*. We previously cloned the ionized calcium-binding adaptor molecule 1 (*Iba1*) gene, which is expressed selectively in microglia/microphages. To generate new transgenic mice to visualize microglia with enhanced green fluorescent protein (EGFP), we here constructed a plasmid carrying EGFP cDNA under control of the *Iba1* promoter. This construct was injected into C57B/6 mouse zygotes, and the *Iba1*-EGFP transgenic line was developed. Fluorescent *in-situ* hybridization analysis revealed that the *Iba1*-EGFP transgene was located on chromosome 11D. No obvious defects were observed during development or in adulthood, and the EGFP fluorescence remained invariant over the course of at least four generations. Judging from the immunoreactivity with anti-Iba1 antibody, all EGFP-positive cells in the adult brain were ramified microglia. In the developing transgenic embryos, EGFP signals were detected as early as embryonic Day 10.5. The most prominent EGFP signals were found in forebrain, spinal cord, eye, foreleg, yolk sac, liver, and vessel walls. At postnatal Day 6, clear EGFP signals were observed in the supra-ventricular corpus callosum, known as “fountain of microglia,” where amoeboid microglia migrate into the brain parenchyma and mature into ramified microglia. *Iba1*-EGFP transgenic mice thus permit observation of living microglia under a fluorescence microscope and provide a useful tool for studying the function of microglia *in vivo*. © 2005 Wiley-Liss, Inc.

**Key words:** Iba1; EGFP; microglia; visualization

Microglia are the resident macrophages in the brain and are thought to modulate the pathologic and regenerative states of the brain by producing a variety of molecules including neurotrophic and neurotoxic factors (Kreutzberg, 1996; Nakajima and Kohsaka, 2001, 2004). Resident microglia have been observed in the developing brain even in 10-day-old embryo (E10) rat brain (Abney et al., 1981; Fedoroff and Hao, 1991). Morphologically, these cells do not have processes, and referred to as amoeboid microglia. The cell density of this population is sustained at low levels before neurogenesis. The

microglia increase in number in association with neurogenesis and subsequent gliogenesis, and develop morphologically. Cumulative evidence has shown that microglia at this stage play a role in the regulation of cell differentiation, cell number, synapse formation, and tissue clearance (Nagata et al., 1993; Hamilton and Rome, 1994; Cammer and Zhang, 1996; Miller and Kaplan, 2001; Farinas et al., 2002; Markus et al., 2002). From this stage until adulthood, they morphologically change into ramified microglia, which have many fine perpendicular processes extending from a few long prolongations, and uniformly disperse throughout the brain. This type of microglia generally has been considered functionally inactive or in a resting state, and they have been regarded as sensor cells whose function is to detect abnormalities or changes in the brain (Kreutzberg, 1996). When the brain is injured or affected by diseases, such as ischemia or neurodegenerative disease, the ramified microglia at the affected site morphologically transform into cells with retracted processes and enlarged cell bodies, and they increase in number (Kreutzberg, 1996). Microglia with this particular cell form are generally referred to as activated or reactive microglia (Streit et al., 1999). The conventional methods that use immunostaining techniques thus have shown that the morphology, cell number, and distribution of the resident microglia change during development and are altered by injury and disease. The process of these changes, however, has not been well understood.

Recent advances in techniques that use enhanced green fluorescent protein (EGFP) to visualize particular cells or protein molecules *in situ* make it possible to investigate cell morphology, the dynamics of target proteins, and their regulation in living tissues and cells. In

Contact grant sponsor: Ministry of Health, Labor and Welfare, Japan; Contract grant sponsor: Japan Health Sciences Foundation.

Y. Imai is currently at the Division of Molecular Cellular Physiology, Department of Molecular Cellular Biology, School of Medicine, Ehime University, Shigenobu, Onsen-gun, Ehime 791-0295, Japan.

\*Correspondence to: Shinichi Kohsaka, Department of Neurochemistry, National Institute of Neuroscience, 4-1-1 Ogawahigashi, Kodaira, Tokyo 187-8502, Japan. E-mail: kohsaka@ncnp.go.jp

Received 2 September 2004; Accepted 15 September 2004

Published online 9 June 2005 in Wiley InterScience (www.interscience.wiley.com). DOI: 10.1002/jnr.20480

combination with genome engineering, generation of the transgenic mice expressing EGFP in target cells is a very useful tool for studying cell properties in situ. For example, transgenic mice carrying EGFP under the control of the astrocyte-specific glial fibrillary acidic protein (GFAP) promoter have revealed the dynamic changes in astrocyte morphology during development (Zhuo et al., 1997; Nolte et al., 2001). In addition, the identification and characterization of neural stem cells not only in embryos but in adult brain has been achieved by using transgenic mice carrying EGFP under the control of the nestin second-intronic enhancer (Kawaguchi et al., 2001; Mignone et al., 2004). We therefore tried to produce transgenic mice in which microglia can be visualized in situ as a means of studying the properties of microglia during development, including changes in morphology, cell number, and distribution.

To achieve this end, we used the promoter of the ionized calcium-binding adaptor molecule 1 (*Iba1*) gene. *Iba1*, which is identical to allograft inflammatory factor-1 (AIF-1) (Utans et al., 1995) and balloon angioplasty responsive transcription-1 (BART-1) (Autieri et al., 1996), is a 17-kDa protein containing two EF-hand motifs, is expressed selectively in microglia/macrophages (Imai et al., 1996). We generated transgenic mice carrying EGFP under the control of the *Iba1* promoter and demonstrated that the microglia/macrophages of these transgenic mice specifically expressed EGFP. In the present study, we developed a valuable tool for visualize microglia/macrophages throughout the body and in living tissue.

## MATERIALS AND METHODS

### Transgene Construction

A genomic gene of mouse *Iba1* was cloned from a 129Sv/J mouse cosmid library (Stratagene; GenBank accession number AB036423). The transgene construct was prepared by subcloning the 1.9-kb *EcoRI*-*HindIII* fragment from the 5'-flanking region of the *Iba1* gene (position 2178–4066), including exon 1, intron 1, and a portion of exon 2, fused with a cDNA of EGFP and a polyadenylation (poly-A) sequence of simian virus 40 from pIRES-EGFP (Clontech, Palo Alto, CA) into the pBluescript II SK(-) vector, generating *Iba1*-EGFP plasmid. This transgene construct was designed to add 17 additional amino acids to the N-terminal of EGFP, whose expression was controlled by the *Iba1* promoter.

### Cell Culture and Transfection

THP-1 cells (a human acute monocytic leukemic cell line, Tsuchiya et al., 1980) and COS-7 (a monkey kidney epithelium cell line) cells were grown in RPMI1640 (Gibco BRL, Grand Island, NY) and Dulbecco's modified Eagle medium (DMEM; Gibco BRL), respectively, containing 10% heat-inactive fetal bovine serum (FBS; Irvine, Santa Ana, CA), at 37°C under a humidified 5% CO<sub>2</sub> atmosphere. For the transient expression studies, THP-1 cells and COS-7 cells were transfected with expression plasmid by electroporation with GenePulser (Bio-Rad) and by using Lipofectamine Plus (Gibco BRL), respectively, as indicated in the manufacturer's protocol.

### Generation and Genotyping of *Iba1*-EGFP Transgenic Mice

Transgenic mice were generated by pronuclear microinjection of fertilized C57BL/6 strain oocytes. To identify founder mice, the genotypes of all offspring were analyzed by polymerase chain reaction (PCR) as follows. Genomic DNA was prepared from tail biopsies. The thermocycle profile for PCR amplification was: 1 min at 94°C, 1 min at 55°C, and 2 min at 72°C for 40 cycles. The primers for PCR analysis were: sense primer for *Iba1* gene and transgene, 5'-TACCGC-ATCCTTGGTTTGAG-3'; anti-sense primer for *Iba1* gene, 5'-CTTGTGGATCCCCCTCCAGCC-3'; and anti-sense primer for transgene, 5'-CTTGTACAGCTCGTCCATGC-3'. The PCR products, a 0.8-kb fragment of the genomic *Iba1* gene and a 1.5-kb fragment of the transgene, were separated on a 0.7% agarose gel and stained with ethidium bromide.

### Fluorescent In Situ Hybridization Analysis

Fluorescent in situ hybridization (FISH) analysis of the chromosomes from the mice was carried out as described previously (Matsuda et al., 1992). Briefly, the cDNA of EGFP was labeled with biotin-16-dUTP with a nick translation kit (Roche, Germany). After overnight hybridization, the signals were detected with fluorescein isothiocyanate (FITC)-conjugated avidin (Roche). Counterstaining was carried out with propidium iodide (PI) and Hoechst 33258.

### Preparation of Living Slices and Microtome Sections

Living slices were prepared as follows. The dissected brain was placed on 3% agarose, then cut into 200- to 400- $\mu$ m sections in ice-cold Tyrode's solution (in mM: 136.8 NaCl, 2.5 KCl, 1.7 CaCl<sub>2</sub>, 1.0 MgCl<sub>2</sub>, 0.38 Na<sub>2</sub>PO<sub>4</sub>, 11.9 NaHCO<sub>3</sub>, and 5.5 glucose) with a microtome VT-1000S (Leica, Germany), and examined with a fluorescence stereoscopic microscope MZFL III (Leica).

Microtome sections were prepared as follows. The dissected brains were fixed with 4% paraformaldehyde (PFA) at 4°C for 16 hr. After washing in phosphate-buffered saline (PBS) for 20 min, the brains were cut into 50- $\mu$ m sections in PBS with a microtome.

The experimental protocols were approved by The Animal Care and Use Committee of National Institute of Neuroscience.

### Immunohistochemistry

The dissected brains were fixed with 4% PFA at 4°C for 16 hr. After washing in PBS for 20 min, the brains were equilibrated in 20% sucrose in PBS, embedded in optimal cutting temperature (OTC) compound, and frozen in dry ice. The frozen brains were cut into 14- $\mu$ m sections with a cryostat CM-3000 (Leica), and the sections were mounted onto 3-aminopropyltriethoxysilane (APS)-coated glass slides (Matsunami, Osaka, Japan). The sections were permeabilized and blocked with 3% goat serum-0.1% Triton X-100 in PBS for 20 min, and then stained with rabbit polyclonal anti-*Iba1* (2  $\mu$ g/ml). After three washes with PBS, the sections were incubated for 1 hr at room temperature with Alexa Fluor594-goat anti-rabbit IgG (H+L, 1:1,000; Molecular Probes, Eugene, OR) in PBS

containing 3% bovine serum albumin. The sections were then mounted on a glass slide with PermaFluor (Thermo Shandon, Pittsburgh, PA) and examined with an AX70 fluorescence microscope (Olympus, Tokyo, Japan).

## RESULTS

### Generation of Iba1-EGFP Transgenic Mice

To obtain the promoter of the mouse *Iba1* gene, we isolated *Iba1* genomic DNA from a 129Sv/J mouse cosmid library. Sequencing analysis revealed that *Iba1* gene consists of six exons, and that five interferon- $\gamma$  (IFN $\gamma$ )-responsive elements (IREs) are present in the upstream of the second exon (Fig. 1A). A previous study showed that the restricted expression of *Iba1* in microglia/macrophage is enhanced by IFN $\gamma$ , suggesting that the expression of *Iba1* is controlled by IRE (Imai and Kohsaka, 2002; Sibinga et al., 2002). To determine whether the *EcoRI-HindIII* 1.9-kb *Iba1* genomic fragment containing IRE shown in Figure 1A functions as a promoter, we constructed a plasmid in which a cDNA of EGFP and a poly-A sequence were placed downstream of the 1.9-kb *Iba1* genomic fragment. Because *Iba1* is expressed in a human acute monocytic leukemia cell line, THP-1 cells, but not in COS-7 cells, the plasmid was introduced into THP-1 cells and COS-7 cells (Imai et al., 1996). As expected, the EGFP fluorescence was detected only in the THP-1 cells (Fig. 1B), indicating that the 1.9-kb *Iba1* genomic fragment was sufficient to function as a promoter in THP-1 cells as well as an endogenous *Iba1* promoter. This observation prompted us to use this construct as a novel marker of microglia in brain to visualize microglia/macrophages. After injection of the construct into C57BL/6 mouse zygotes, seven transgenic lines were obtained. One line determined by genotyping analysis and EGFP fluorescence was then chosen for subsequent analysis. No obvious defects were detected during development or in adulthood, and the EGFP fluorescence remained invariant over the course of at least four generations. We then carried out FISH analysis to identify the site where the *Iba1-EGFP* transgene had been integrated into the chromosomes, and as shown in Figure 1C, the twin-spot FITC signals of the *Iba1-EGFP* transgene were detected on chromosome 11D.

### EGFP-Positive Cells in the Adult Brain of Iba1-EGFP Transgenic Mice Were Identified As Microglia

We initially examined the living brain slices prepared from the adult *Iba1-EGFP* transgenic mice for EGFP fluorescence. Under a simple light transmission mode at low magnification, the slices appeared bright but when the same field was illuminated with a laser beam, they emitted strong diffuse fluorescence (Fig. 2A). The slices prepared from the nontransgenic mice, however, showed no signals (data not shown), indicating that the observed fluorescence was the EGFP signal, not autofluorescence. At higher magnification, fluorescence was observed throughout the brain slices and matched

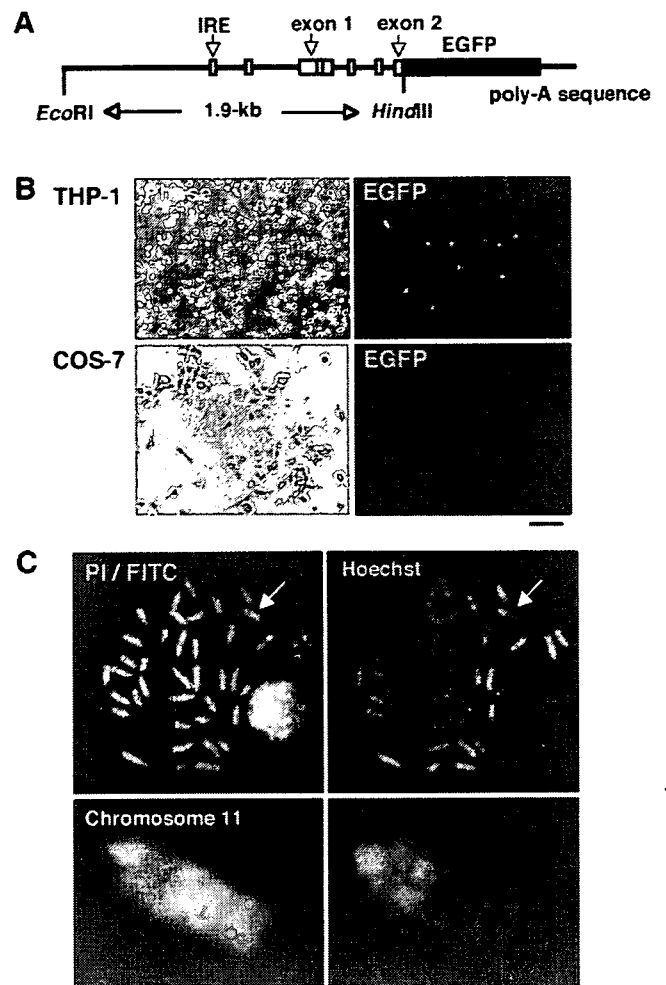


Fig. 1. *Iba1*-enhanced green fluorescent protein (EGFP) transgenic mice. **A:** Schematic of the *Iba1-EGFP* transgene construct. The 1.9-kb *EcoRI-HindIII* fragment from the 5'-flanking region of *Iba1* gene including exon 1, intron 1, and a portion of exon 2 was fused with EGFP cDNA (black box) and a polyadenylation sequence. The five red boxes represent the interferon- $\gamma$  responsive elements (IREs). **B:** Transfection of the *Iba1-EGFP* transgene construct into THP-1 cells and COS-7 cells. A phase-contrast image (left panel) and EGFP fluorescence image (right panel) are shown. Scale bar = 50  $\mu$ m. **C:** Fluorescent in situ hybridization (FISH) analysis. The chromosomal location of *Iba1-EGFP* transgene is indicated by the arrow. The left panels show the FITC signals, indicating that the *Iba1-EGFP* transgene merged with R-banded chromosomes stained with propidium iodide (PI). The right panels show G-banded chromosomes stained with Hoechst 33258 (Hoechst). The lower panels show chromosome 11 at higher magnification.

the distribution of microglia detected by immunostaining (Fig. 2B). When examined with a 40 $\times$  objective, the cells emitting EGFP fluorescence were concluded to be ramified microglia based on their morphology (Fig. 2C).

We next investigated whether EGFP expression in the brain is controlled precisely by the *Iba1* promoter by carrying out an immunohistochemical analysis with anti-*Iba1* antibody. As shown in Figure 2D, the EGFP-positive cells were observed uniformly throughout the brain,

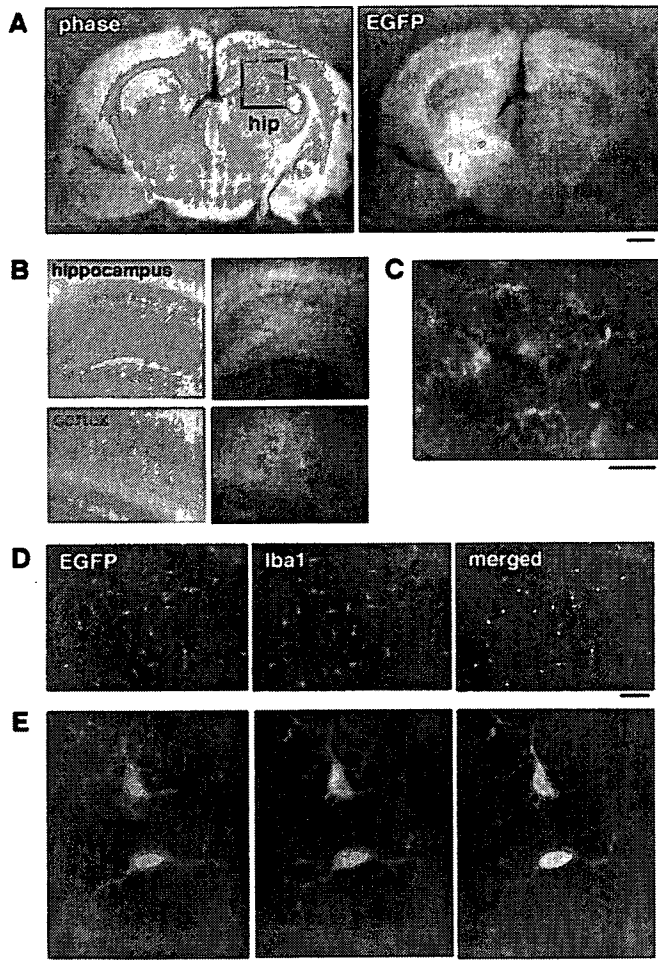


Fig. 2. Enhanced green fluorescent protein (EGFP) fluorescence in the brain of adult Iba1-EGFP transgenic mice. **A:** Microtome section. A phase-contrast image (left panel) and EGFP fluorescence image (right panel) are shown. Scale bar = 1 mm. hip, hippocampus; cx, cortex. **B:** Hippocampus and cortex enclosed by boxes in A are shown at higher magnification. A phase-contrast image (left panel) and EGFP fluorescence image (right panel) are shown. **C:** EGFP-positive cells in the cortex are shown at higher magnification. Scale bar = 50  $\mu$ m. **D, E:** Microphotographs of immunohistochemically stained brain section with anti-Iba1 antibody. EGFP-positive cells completely matched with Iba1-expressing ramified microglia. Scale bar = 100  $\mu$ m (D); 25  $\mu$ m (E).

and all were immunoreactive for anti-Iba1 antibody. At higher magnification, the EGFP-expressing cells were found to be typical ramified microglia (Fig. 2E). EGFP expression in the Iba1-EGFP transgenic mice thus paralleled Iba1 expression in the adult brain. Because Iba1 is expressed selectively in microglia, we concluded that the *Iba1-EGFP* transgene was expressed in microglia.

#### EGFP Expression in the Transgenic Mice During Development

EGFP signals were detected in the developing Iba1-EGFP transgenic embryos as early as E10.5 (Fig. 3A). At

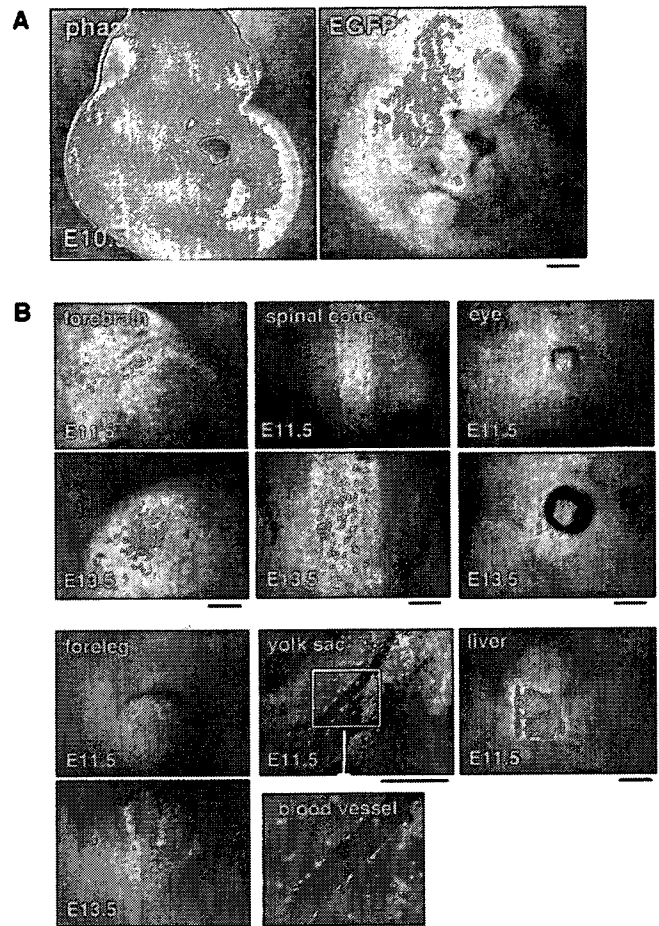


Fig. 3. Enhanced green fluorescent protein (EGFP) fluorescence in Iba1-EGFP transgenic mouse embryos. **A:** Whole embryonic Day 10.5 (E10.5) embryo. A phase-contrast image (left panel) and EGFP fluorescence image (right panel) are shown. Scale bar = 500  $\mu$ m. **B:** EGFP fluorescence images in specific regions at E11.5 and E13.5 embryos. Forebrain, spinal cord, eye, foreleg, yolk sac, and liver are shown. The blood vessel enclosed in yolk sac is shown at higher magnification. Scale bar = 500  $\mu$ m.

E11.5, prominent EGFP signals were observed in the forebrain, spinal cord, eye, foreleg, yolk sac, liver, and vessel walls. As embryonic development proceeded, the intensity of EGFP fluorescence gradually increased from day to day (Fig. 3B). At this stage, the EGFP-positive cells in the brain were distributed mainly on the pial surface.

In the early postnatal stage, microglial cells invade the brain from specific areas, such as the supraventricular corpus callosum. These invading amoeboid microglia migrate into the brain parenchyma where they ultimately mature to ramified microglia (Imamoto and Leblond, 1978; Ling, 1979). We then examined the EGFP signals in the Iba1-EGFP transgenic mice at postnatal Day 6 (P6). As shown in Figure 4A, clear EGFP signals were observed in the supraventricular corpus callosum, and morphologically the EGFP-positive cells were the amoeboid type (Fig. 4B). As development proceeded, the

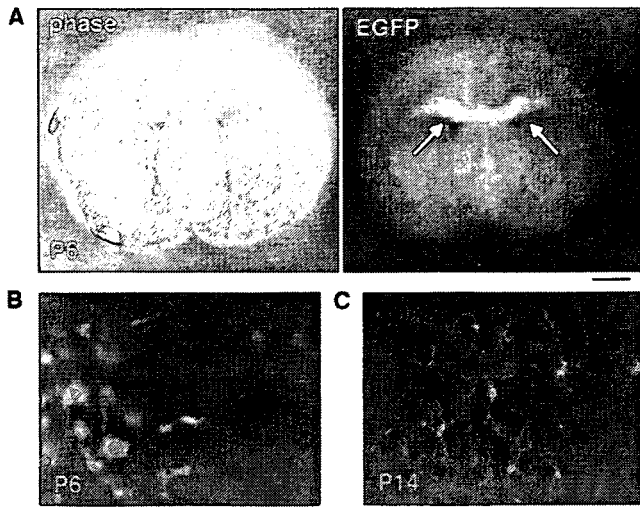


Fig. 4. Enhanced green fluorescent protein (EGFP) fluorescence in Iba1-EGFP transgenic mice. **A:** Microtome section at mouse stage postnatal Day 6 (P6). A phase-contrast image (left panel) and EGFP fluorescence image (right panel) are shown. The supraventricular corpus callosum is indicated by arrows. Scale bar = 1 mm. **B, C:** EGFP-positive cells in the supraventricular corpus callosum in a P6 (**B**) and in the cortex in a P14 (**C**) mouse are shown at higher magnification. Scale bar = 50  $\mu$ m.

EGFP-positive cells in this area decreased in number, and eventually failed to be detected in the P14 transgenic mice (data not shown), and the EGFP-positive cells in the cortical parenchyma became mature ramified microglia (Fig. 4C).

## DISCUSSION

Immunostaining with antibody is a conventional technique for studying the properties of microglia. Because its application is restricted to fixed tissues, i.e., dead cells, however, it is difficult to identify accurately dynamic changes in developing microglia. To overcome this problem, we generated transgenic mice with expression of EGFP under the control of the *Iba1* promoter. Because this promoter selectively functions in microglia/macrophages (Imai et al., 1996), microglia/macrophages in living tissues can be labeled with EGFP fluorescence. To verify that the EGFP-expressing cells in the brain were indeed microglia, we immunostained the same sections for Iba1 and confirmed that all EGFP-expressing cells were also labeled with anti-Iba1 antibody. We therefore concluded that the Iba1-EGFP transgenic mice permit visualization of microglia in living brain tissue.

It is well known that amoeboid microglia, which exhibit immature features, migrate through the brain parenchyma during differentiation and transform into mature ramified microglia when they reach their final location (Ling and Wong, 1993; Cuadros and Navascués, 1998; Dalmau et al., 2003). We used Iba1-EGFP transgenic mice to confirm that EGFP-positive cells in the brain in the embryonic stage were of the amoeboid form, but were of the ramified form in adult brain. Despite

great effort, however, the ontogenesis of microglia remains a matter of controversy and awaits elucidation. Previous reports have led to two hypotheses for the origin of microglia: a neuroectodermic origin and a mesodermal origin. In the latter hypothesis, hematopoietic cell-derived precursors, such as primitive macrophages and monocytes, have been proposed as the cells of origin of microglia. These cells are thought to enter the developing brain from the bloodstream, the ventricular spaces, or the meninges (Ling and Wong, 1993; Cuadros and Navascués, 1998, 2001; Dalmau et al., 2003). The Iba1-EGFP transgenic mice allow visualization of microglia after E10.5. The yolk sac and liver were among the organs that emitted prominent EGFP fluorescence, corroborating the results of a previous study showing that microglial progenitors originate from the yolk sac and are carried to the brain from hematopoietic organs, such as the liver, by the bloodstream (Alliot et al., 1999). In the embryonic stage, the EGFP-positive cells in the brain were detected mainly on the pial surface, and this finding is consistent with the proposal that the meninges is one of the entry routes for microglia into the brain parenchyma (Cuadros and Navascués, 1998). Although microglia mainly invade the brain parenchyma in the prenatal period, a smaller population invades postnatally, at P5–10. This late invasion is restricted to particular areas, such as the cingulum and the supraventricular corpus callosum, which is known to represent a “fountain of microglia” (Imamoto and Leblond, 1978; Ling, 1979). Using the Iba1-EGFP transgenic mice at P6 in this study enabled us to confirm that the strong EGFP signals originated in the amoeboid microglia in the supraventricular corpus callosum. The living tissues of Iba1-EGFP transgenic mice can thus be used to analyze the ontogenesis of microglia. We also believe that they will be useful for visualizing dynamic changes in microglia during physiologic processes, such as cell proliferation and phagocytic behavior, in real time.

Iba1-EGFP transgenic mice exhibited different phenotypes of EGFP fluorescence depending on their parental origin. The mice carrying the paternally inherited transgene displayed a robust EGFP signal, whereas the mice carrying the maternally inherited transgene displayed little or no signal. FISH analysis revealed that the *Iba1-EGFP* transgene was located on chromosome 11D, where it has been suggested to be imprinted (Monk et al., 2003). Although the cause of the different phenotypes is unclear, the differential expression of the *Iba1-EGFP* transgene may be caused by intrinsic genomic imprinting of the *Iba1* gene. Further study will be needed to answer this question.

## ACKNOWLEDGMENTS

We thank Dr. K. Goto (Central Institute for Experimental Animals) for help with the FISH analysis, and Dr. T. Kubota (University of Yamanashi) for valuable discussion and advice.

## REFERENCES

- Abney ER, Bartlett PP, Raff MC. 1981. Astrocytes, ependymal cells, and oligodendrocytes develop on schedule in dissociated cell cultures of embryonic rat brain. *Dev Biol* 83:301–310.
- Alliot F, Godin I, Pessac B. 1999. Microglia derive from progenitors, originating from the yolk sac, and which proliferate in the brain. *Brain Res Dev Brain Res* 117:145–152.
- Autieri MV, Prystowsky MB, Ohlstein EH. 1996. Isolation and characterization of BART-1: a novel balloon angioplasty responsive transcript in rat carotid arteries. *DNA Cell Biol* 15:297–304.
- Cammer W, Zhang H. 1996. Carbonic anhydrase II in microglia in fore-brains of neonatal rats. *J Neuroimmunol* 67:131–136.
- Cuadros M, Navascués J. 1998. The origin and differentiation of microglial cells during development. *Prog Neurobiol* 56:173–189.
- Cuadros M, Navascués J. 2001. Early origin and colonization of the developing central nervous system by microglial precursors. In: Castellano B, Nieto-Sampedro M, editors. *Glial cell function*. Amsterdam: Elsevier. p 51–59.
- Dalmau I, Vela JM, González B, Finsen B, Castellano B. 2003. Dynamics of microglia in the developing rat brain. *J Comp Neurol* 458:144–157.
- Farinas I, Cano-Jaimez M, Bellmunt E, Soriano M. 2002. Regulation of neurogenesis by neurotrophins in developing spinal sensory ganglia. *Brain Res Bull* 57:809–816.
- Fedoroff S, Hao C. 1991. Origin of microglia and their regulation by astroglia. *Adv Exp Med Biol* 296:135–142.
- Hamilton SP, Rome LH. 1994. Stimulation of in vitro myelin synthesis by microglia. *Glia* 11:326–335.
- Imai Y, Ibata I, Ito D, Ohsawa K, Kohsaka S. 1996. A novel gene *iba1* in the major histocompatibility complex class III region encoding an EF hand protein expressed in a monocytic lineage. *Biophys Biochem Res Commun* 224:855–862.
- Imai Y, Kohsaka S. 2002. Intracellular signaling in M-CSF-induced microglial activation: role of *Iba1*. *Glia* 40:164–174.
- Imamoto K, Leblond CP. 1978. Radioautographic investigation of gliogenesis in the corpus callosum of young rat. II. Origin of microglial cells. *J Comp Neurol* 180:139–164.
- Kawaguchi A, Miyata T, Sawamoto K, Takashita N, Murayama A, Akamatsu W, Ogawa M, Okabe M, Tano Y, Goldman SA, Okano H. 2001. Nestin-EGFP transgenic mice: visualization of the self-renewal and multipotency of CNS stem cells. *Mol Cell Neurosci* 17:259–273.
- Kreutzberg GW. 1996. Microglia: a sensor for pathological events in the CNS. *Trends Neurosci* 19:312–318.
- Ling EA. 1979. Transformation of monocytes into ameboid microglia in the corpus callosum of postnatal rats, as shown by labeling monocytes by carbon particles. *J Anat* 128:847–858.
- Ling EA, Wong WC. 1993. The origin and nature of ramified and ameboid microglia: a historical review and current concepts. *Glia* 7:9–18.
- Markus A, Patel TD, Snider WD. 2002. Neurotrophic factors and axonal growth. *Curr Opin Neurobiol* 12:523–531.
- Matsuda Y, Harada YN, Natsune-Sakai S, Lee K, Shiomi T, Chapman VM. 1992. Location of the mouse complement factor H gene (*cfh*) by FISH analysis and replication R-banding. *Cytogenet Cell Genet* 61:282–285.
- Mignone JL, Kukekov V, Chiang AS, Steindler D, Enikolopov G. 2004. Neural stem and progenitor cells in nestin-GFP transgenic mice. *J Comp Neurol* 469:311–324.
- Miller FD, Kaplan DR. 2001. Neurotrophin signaling pathways regulating neuronal apoptosis. *Cell Mol Life Sci* 58:1045–1053.
- Monk D, Smith R, Arnaud P, Preece MA, Stanier P, Beechey CV, Peters J, Kelsey G, Moore GE. 2003. Imprinted methylation profiles for proximal mouse chromosomes 11 and 7 as revealed by methylation-sensitive representational difference analysis. *Mamm Genome* 14:805–816.
- Nagata K, Takei N, Nakajima K, Saito H, Kohsaka S. 1993. Microglial conditioned medium promotes survival and development of cultured mesencephalic neurons from embryonic rat brain. *J Neurosci Res* 34:357–363.
- Nakajima K, Kohsaka S. 2001. Microglia: activation and their significance in the central nervous system. *J Biochem* 130:169–175.
- Nakajima K, Kohsaka S. 2004. Microglia: neuroprotective and neurotrophic cells in the central nervous system. *Curr Drug Targets Cardiovasc Haematol Disord* 4:65–84.
- Nolte C, Matyash M, Pivneva T, Schipke CG, Ohlemeyer C, Hanisch UK, Kirchhoff F, Kettenmann H. 2001. GFAP promoter-controlled EGFP-expressing transgenic mice: a tool to visualize astrocytes and astrogliosis in living brain tissue. *Glia* 33:72–86.
- Sibinga NE, Feinberg MW, Yang H, Werner F, Jain MK. 2002. Macrophage-restricted and interferon  $\gamma$ -inducible expression of the allograft inflammatory factor-1 gene requires Pu.1. *J Biol Chem* 277:16202–16210.
- Streit WJ, Walter SA, Pennell NA. 1999. Reactive microgliosis. *Prog Neurobiol* 57:563–581.
- Tsuchiya S, Yamabe M, Yamaguchi Y, Kobayashi Y, Konno T, Tada K. 1980. Establishment and characterization of a human acute monocytic leukemia cell line (THP-1). *Int J Cancer* 26:171–176.
- Utans U, Arceci RJ, Yamashita Y, Russell ME. 1995. Cloning and characterization of allograft inflammatory factor-1: a novel macrophage factor identified in rat cardiac allografts with chronic rejection. *J Clin Invest* 95:2954–2962.
- Zhuo L, Sun B, Zhang CL, Fine A, Chiu SY, Messing A. 1997. Live astrocytes visualized by green fluorescent protein in transgenic mice. *Dev Biol* 187:36–42.

# Ubiquitylation and Degradation of Serum-inducible Kinase by hVPS18, a RING-H2 Type Ubiquitin Ligase\*

Received for publication, August 1, 2005, and in revised form, September 15, 2005. Published, JBC Papers in Press, October 3, 2005, DOI 10.1074/jbc.M508397200

Satomi Yogosawa<sup>‡§</sup>, Shigetsugu Hatakeyama<sup>¶</sup>, Keiichi I. Nakayama<sup>||</sup>, Hiroyuki Miyoshi<sup>\*\*</sup>, Shinichi Kohsaka<sup>+1</sup>, and Chihiro Akazawa<sup>‡</sup>

From the <sup>‡</sup>Department of Neurochemistry, National Institute of Neuroscience, National Center of Neurology and Psychiatry, Tokyo 187-8502, Japan, <sup>§</sup>Division of Molecular Life Science, School of Life Science, Tokyo University of Pharmacy and Life Science, Tokyo 192-0392, <sup>¶</sup>Department of Molecular Biochemistry, Hokkaido University Graduate School of Medicine, Sapporo 060-8638, <sup>||</sup>Department of Molecular and Cellular Biology, Medical Institute of Bioregulation, Kyushu University, CREST, Japan Science and Technology Agency, Fukuoka 812-8582, <sup>\*\*</sup>Subteam for Manipulation of Cell Fate, Bio Resource Center, RIKEN, Tsukuba 305-0074, Japan

Serum-inducible kinase (SNK) is a member of polo-like kinases that serve as regulators of multiple events during cell division. Rapid changes in the activity and abundance of SNK were reported after the serum stimulation and after the activation of synaptic transmission in the brain. Yet the detailed mechanisms that control the level of SNK protein have not been fully elucidated. In this report, we show that the RING-H2 domain of hVPS18 (human vacuolar protein sorting 18) has a genuine ubiquitin ligase (E3) activity. Using the yeast two-hybrid screening, we identify SNK as a candidate substrate of hVPS18. The half-life of SNK is increased in HeLa cells that down-regulated hVPS18 by lentivirus-mediated small hairpin RNA interference. Furthermore, the delayed entry into S phase is observed in HeLa cells overexpressing hVPS18. These results suggest that hVPS18 may play an important role in regulation of SNK activity through its ubiquitin ligase.

The polo-like kinases are a family of serine/threonine protein kinases that include mammalian polo-like kinase (Plk)1,<sup>2</sup> SNK (Plk2), fibroblast growth factor (Plk3), Sak (Plk4), *Caenorhabditis elegans* Plc1–3, *Xenopus laevis* Plx1, *Drosophila* polo, fission yeast Plo1, and budding yeast Cdc5 (1). Genetic and biochemical evidence in various organisms indicates that polo-like kinases play pivotal roles in regulating many cell-cycle dependent processes such as centrosome maturation and separation, mitotic entry, metaphase to anaphase transition, mitotic exit, and cytokinesis (2, 3). A number of studies (4, 5) suggest that the kinase activity is regulated by a variety of post-translational processes, including phosphorylation and ubiquitin conjugation.

The mammalian homologues of yeast Class C type of vacuolar protein sorting (VPS) proteins appear to control the fusion events of late endosomes and lysosomes that are the major pathway of the intracellular protein degradation (6, 7). There are four genes in human Class C VPS: hVPS11, hVPS16, hVPS18, and hVPS33. Studies of the domains of

hVPS11 and hVPS18 have consistently revealed the existence of a RING-H2 motif, a member of RING fingers, located near the C-terminal. RING-H2 finger domains are present in a wide variety of proteins, and in the recent past it has been found that several RING-H2 finger proteins take part in the ubiquitin-proteasome pathway by playing as E3 ubiquitin ligases. The ubiquitin conjugation has been implicated in a variety of cellular processes, including cell-cycle control, signal transduction, transcriptional regulation, and cell death (8, 9). Furthermore, the conjugation with ubiquitin also serves as a sorting signal that determines the destination of various proteins at the different subcellular organelles such as the plasma membrane, the trans-Golgi network, and the endosome (10). The conjugation of ubiquitin to substrate proteins requires at least three enzymes: the ubiquitin-activating enzyme (E1), a ubiquitin-conjugating enzyme (E2), and a ubiquitin ligase (E3). The RING-H2 finger is a zinc binding domain with an octet of cysteines and histidines with a defined space representing the largest class of ubiquitin ligases to date. For instance, mammalian genomes encode hundreds of RING finger proteins, and it has not yet been clear whether all of these proteins have E3 activity or not (11). In this regard, a number of molecules are waiting for characterization that may help us to understand how the intracellular protein levels are controlled. Despite the recent investigation of the Class C VPS in the membrane traffic of the yeast and mammals, the molecular mechanisms remain undefined. In this report, we demonstrate that hVPS18 is a genuine ubiquitin ligase E3 and search in the rat brain for interacting molecules with hVPS18 using the yeast two-hybrid screen. Here we identified SNK as one of the candidate substrates of the ubiquitin ligase activity of hVPS18.

## MATERIALS AND METHODS

**Yeast Two-hybrid Screen and cDNA Cloning**—For the yeast two-hybrid screen, the yeast strain AH109 was transformed sequentially with pGBKT7-hVPS18, as a bait, and a cDNA library of the rat brain (BD Biosciences Clontech) using the lithium acetate method. We screened  $2 \times 10^6$  transformants on the plate containing synthetic dropout medium lacking histidine, tryptophan, and leucine. Positive clones were selected on 5 mM 3-aminotriazole-containing medium lacking leucine, tryptophan, and histidine and verified with a filter assay for  $\beta$ -galactosidase activity. The prey plasmids were recovered and sequenced. The full-length SNK was isolated by reverse transcription-PCR from the rat brain cDNA. We assessed the interaction of hVPS18 and rat SNK in AH109 cells transformed sequentially with pGBKT7-hVPS18 (full-length or  $\Delta$ RING) and pGADT7 containing SNK or clone #A12–1 by quantifying  $\beta$ -galactosidase activity.

\* This work was funded by Ministry of Health, Labor, and Welfare, Japan and by a grant-in-aid for Scientific Research from the Ministry of Education, Science, Sports and Culture of Japan. The costs of publication of this article were defrayed in part by the payment of page charges. This article must therefore be hereby marked "advertisement" in accordance with 18 U.S.C. Section 1734 solely to indicate this fact.

<sup>1</sup> To whom correspondence should be addressed. Tel.: 81-423-41-2711; Fax: 81-423-46-1751; E-mail: kohsaka@ncnp.go.jp.

<sup>2</sup> The abbreviations used are: Plk, polo-like kinase; VPS, vacuolar protein sorting; SNK, serum-inducible kinase; PBD, polo-box domain; E1, ubiquitin-activating enzyme; E2, ubiquitin-conjugating enzyme; E3, ubiquitin ligase; shRNA, short hairpin RNA; CMV, cytomegalovirus; HA, hemagglutinin; hVPS, human VPS; DMEM, Dulbecco's modified Eagle's medium; BrdU, bromodeoxyuridine; ERK, extracellular signal-regulated kinase; SPAR, spine-associated Rap guanosine triphosphatase (GTPase)-activating protein; NHS, N-hydroxysuccinimide.



## Ubiquitylation of SNK by hVPS18

**Plasmid Construction**—Full-length and various truncated SNK cDNAs were subcloned into the following vectors: the pGEX-4T2 (Amersham Biosciences) prokaryotic expression vector for the production of GST-tagged fusion proteins; the pCMV-HA, pCMV-FLAG, and pCMV-Myc mammalian expression vectors (BD Biosciences Clontech) for the production of HA-tagged, FLAG-tagged, and Myc-tagged fusion proteins. Myc-tagged and HA-tagged hVPSs (hVPS11, hVPS18, hVPS18 $\Delta$ RING, hVPS16, and hVPS33a) mammalian expression vectors were prepared as described previously (6). The full-length hVPSs (hVPS11, hVPS18, and hVPS16) were subcloned into pFastBacHTb insect expression vector (Invitrogen) to generate His-tagged hVPSs.

**Expression and Preparation of Recombinant Proteins**—Ubiquitin-conjugating enzymes (E2s) were expressed in *E. coli* strain BL21-AI (Invitrogen) and lysed in a buffer containing phosphate-buffered saline, 1 mM phenylmethylsulfonyl fluoride, and Complete protease inhibitor mixture (Roche Molecular Biochemicals). The supernatant, after centrifugation at 14,000  $\times g$  for 10 min, was used for the ubiquitylation reaction. Full-length and various truncated mutants of GST-SNK were expressed in *E. coli* strain BL21-AI, and the recombinant proteins were purified using glutathione-Sepharose 4B beads (Amersham Biosciences) in phosphate-buffered saline, 1 mM phenylmethylsulfonyl fluoride, Complete protease inhibitor mixture. His-tagged hVPSs (hVPS11, hVPS18, and hVPS16) were expressed in Sf9 insect cells using baculovirus protein expression system (Invitrogen), and the recombinant proteins were purified by using ProBond metal affinity beads (Invitrogen) in a buffer containing 50 mM Tris-HCl, pH 7.4, 3 mM MgCl<sub>2</sub>, 0.1% Nonidet P-40, 1 mM phenylmethylsulfonyl fluoride, 200 mM NaCl.

**Cell Culture and DNA Transfection**—COS7, HeLa, and HEK293T cells were maintained in Dulbecco's modified Eagle's medium (DMEM) supplemented with 10% fetal bovine serum, 100 units/ml penicillin, and 100  $\mu$ g/ml streptomycin in humidified incubators with 5% CO<sub>2</sub> at 37 °C. The cells were transfected with various plasmids by FuGENE 6 reagent (Roche Molecular Biochemicals) according to the manufacturer's instructions.

**Antibodies**—His-tagged full-length rat SNK was expressed in Sf9 cells. The protein was purified by ProBond metal affinity resin and used as immunogens in Wistar rats. The affinity purification using His-SNK coupled to a HiTrap NHS-activated column (Amersham Biosciences) was performed according to the manufacturer's instruction. The rabbit anti-SNK polyclonal antibody was kindly provided by Dr. M. H. Sheng. Anti-hVPS antibodies (hVPS11, hVPS16, and hVPS18) were prepared as described previously (6). Other antibodies used were as follows: mouse monoclonal anti-Myc antibody (9E10, Roche Molecular Biochemicals), rat monoclonal anti-HA antibody (3F10, Roche Molecular Biochemicals), mouse monoclonal anti-FLAG (M2)-agarose (Sigma), rabbit polyclonal anti-ubiquitin antibody (Sigma), and mouse monoclonal anti- $\alpha$ -tubulin antibody (B-5-1-2, Sigma).

**Immunoprecipitation**—For immunoprecipitation, the cells were lysed in modified radioimmune precipitation assay buffer (50 mM Tris, pH 7.6, 250 mM NaCl, 1% Triton X-100, 3 mM EDTA) supplemented with Complete protease inhibitor mixture. Total cell lysates were centrifuged at 10,000  $\times g$  for 10 min, and the protein concentration of the supernatants was determined. Identical amounts of the protein from each sample were precleared by incubation with protein A/G Sepharose 4 fast flow (Amersham Biosciences) for 30 min at 4 °C. After the removal of protein A/G-Sepharose by brief centrifugation, the solution was incubated with 2  $\mu$ g of monoclonal anti-Myc antibody, monoclonal anti-HA antibody, or control IgGs at 4 °C overnight. Immunoprecipitation of the antigen-antibody complex was accomplished by adding 40  $\mu$ l of protein

A/G-Sepharose for 1 h at 4 °C. Sepharose-bound proteins were solubilized in 40  $\mu$ l of SDS sample buffer. Samples were boiled and separated by SDS-PAGE, and Western blot analyses were performed.

**In Vitro Pull-down Assay**—Full-length and various truncated mutants of GST-SNK were immobilized on glutathione-Sepharose 4B beads and equilibrated with wash buffer (50 mM Tris-HCl, pH 7.4, 150 mM NaCl, 0.1% Triton X-100, 3 mM MgCl<sub>2</sub>, 0.1 mM phenylmethylsulfonyl fluoride) for three times. The resin was incubated with His-tagged hVPSs at 25 °C for 30 min and washed with the wash buffer for three times. The resin was subjected to SDS-PAGE, and Western blot analyses were performed by either anti-hVPS18 antibody, anti-hVPS11 antibody, or anti-hVPS16 antibody.

**In Vivo and in Vitro Ubiquitylation Assay**—Myc-tagged hVPS18, hVPS11, hVPS16, FLAG-tagged SNK, and HA-tagged ubiquitin were co-transfected to COS7 cells using FuGENE 6. Transfected cells were treated with 30  $\mu$ M MG132 for 3 h at 16 h post-transfection. Immunoprecipitation was performed by using anti-FLAG (M2)-agarose, and conjugated HA-ubiquitin was detected by Western blot analyses using anti-HA antibody.

An *in vitro* ubiquitylation assay was performed as described previously (12). GST-SNK full-length was mixed with yeast E1 (500 ng, Boston Biochem), E2-enzyme mixture (Boston Biochem), or UbcH4, ubiquitin (10  $\mu$ g, Boston Biochem) and His-hVPS18. The mixture was incubated at 25 °C for 30 min in the presence of 50 mM Tris-HCl, pH 7.4, 5 mM MgCl<sub>2</sub>, 2 mM dithiothreitol, and 2 mM ATP in a 50- $\mu$ l volume. After incubation, the mixture was subjected to SDS-PAGE and detected by Western blot analyses using anti-GST antibody, anti-ubiquitin antibody, or anti-hVPS18 antibody.

**Establishment of HeLa Cell Lines Up-regulates/Down-regulates hVPS18 by Lentivirus Vector**—The lentivirus containing full-length of hVPS18 or short hairpin RNA (shRNA) interference was raised by the method previously described (13). Briefly, synthetic oligonucleotides (top-strand: 5'-GATCCCCAGGTGTCCATCTTCGCAAAGCGTGTGCTGTCCGCTTTGTGAAGATGGGCACCTTTTTTTGGAAAT-3'; bottom-strand: 5'-CTAGATTTCCAAAAAAGTGCCCATCTT-CACAAAGCGGACAGCACACGCTTTGCGAAGATGGACACCTGGG-3'; underline, loop sequence) were annealed and ligated into the BglII-XbaI site of pENTR4-H1. The full length of hVPS18 cDNA was ligated into the EcoRI-XhoI site of pENTR3C. Then either pENTR4-H1-hVPS18-shRNA or pENTR3C/hVPS18 was incubated with pLent6/V5 DEST (Invitrogen) in the presence of Gateway LR Clonase (Invitrogen) for plasmid recombination. To obtain recombinant lentivirus, the Clonase-recombined plasmid was co-transfected with packaging construct (pCAG-HIVgp), and vesicular stomatitis virus G glycoprotein-expressing, Rev-expressing construct (pCMV-VSV-G-RSV-Rev) to HEK293T cells. The titer of virus was determined by measuring the amount of human immunodeficiency virus, type 1 p24 gag antigen using an enzyme-linked immunosorbent assay kit (PerkinElmer Life Sciences). The recombinant lentivirus (titer: 5  $\times 10^7$  IU/ml) was infected to HeLa cells with 10  $\mu$ g/ml Blasticidin S (Invitrogen) to select the virus-infected cells. The Blasticidin S-resistant colony was identified and expanded to establish the HeLa cell lines that constitutively over-express hVPS18 (HeLa-hVPS18(OE)) or constitutively knock-down hVPS18 by shRNA interference (HeLa-hVPS18(shRNA)). To confirm the expression level of hVPS18 and SNK in the established HeLa cell lines, Western blot analyses and immunocytochemistry were performed as previously described (6).

**[<sup>35</sup>S]Methionine and [<sup>35</sup>S]Cysteine Pulse-chase Analysis**—Three lines of HeLa cells (Control, hVPS18(OE), and hVPS18(shRNA)) were subjected to the *in vivo* pulse-chase analyses using [<sup>35</sup>S]methionine/



[<sup>35</sup>S]cysteine. Each cell was washed with phosphate-buffered saline three times and incubated for 1 h with Met(-)/Cys(-)-DMEM without serum. The medium was then replaced with Met(-)/Cys(-)-DMEM containing 1 mCi of [<sup>35</sup>S]Met/[<sup>35</sup>S]Cys Express Protein Labeling Mixture (Amersham Biosciences) and 10% fetal bovine serum. After incubation for 2 h, the medium was replaced with non-radioactive DMEM complete medium. Cells were then incubated for indicated chase time and harvested. Cells were lysed and immunoprecipitated, using anti-SNK antibody and protein A/G-Sepharose 4 fast flow. Immunoprecipitates were subjected to SDS-PAGE and detected by BAS5000 image analyzer (FUJI Film).

**Flow Cytometric Analysis**—Cell cycle of HeLa cells was synchronized and released from G<sub>1</sub>/S arrest. Briefly, the cells were treated with 3 μg/ml aphidicolin and serum starvation for 14 h. Then, the cells were stimulated to progress the cell cycle by with 10% serum in the absence of aphidicolin for the indicated times. Prior to each harvest, the cells were labeled for 30 min in the presence of BrdUrd at the concentration of 10 μM. For immunostaining of BrdUrd-incorporated DNA, cells were treated as recommended by the manufacturer (BrdU Flow Kit, BD Biosciences). Subsequently, cells were stained with propidium iodide and subjected to fluorescence-activated cell sorting analyses based on DNA content. The each sample (1 × 10<sup>6</sup> cells) was analyzed by the cell-cycle distribution using FACStar cell sorter (BD Bioscience).

## RESULTS

**RING-H2 Domain of hVPS18 Has a Ubiquitin Ligase Activity**—It has been shown that hVPS18, a member of Class C VPS protein, has a RING-H2 finger domain in its C-terminal region (6). To examine whether hVPS18 has a ubiquitin ligase activity, we performed *in vitro* ubiquitylation assay using an *E. coli* lysate as an anonymous substrate. Because Nedd4 has a HECT (homologous to E6-associated protein carboxy terminus) type ubiquitin ligase activity, we used Nedd4 as a positive control of E3 activity (Fig. 1A, lane 7). As shown in Fig. 1A, the ubiquitylated proteins were detected in the presence of E1, E2-enzyme mixture, hVPS18, ubiquitin (Fig. 1A, lane 6) but not detected in the absence of either E1, E2, hVPS18, or *E. coli* lysate (Fig. 1A, lanes 1–5). Therefore, hVPS18 has a ubiquitin ligase activity using bacterial proteins as substrates. In a series of ubiquitylation pathways, it is required for the specific interaction between E3, E2, and substrate, to transfer ubiquitins to a target substrate. To examine the selectivity and the specificity of E2 enzymes for hVPS18, we performed *in vitro* ubiquitylation assay using various E2 enzymes. As shown in Fig. 1B, hVPS18 has a preference for UbcH4 (Fig. 1B, lane 5). Moreover, we examine whether RING-H2 domain of hVPS18 is responsible for ubiquitin ligase activity. As shown in Fig. 1C, hVPS18ΔRING does not have ubiquitin ligase activity *in vitro* (Fig. 1C, lane 3), suggesting that VPS18 functions as a ubiquitin ligase depending on its RING-H2 domain.

**Identification of SNK That Interacts with hVPS18**—To explore the interacting proteins with hVPS18, we screened the rat brain cDNA library by yeast two-hybrid using the full-length human hVPS18 cDNA as a bait. From the screening of 2 × 10<sup>6</sup> clones, we obtained some rat clones encoding the homologues of hVPS11, hVPS16, and hVPS33a (data not shown), that have been shown to constitute a hetero-oligomeric complex with hVPS18, confirming the validity of this screen. Four of the positive clones, two identical clones (clone #A12-1, Fig. 2A) and two independents, have a sequence identity with the rat SNK cDNA (accession number: NM\_031821), which was previously characterized as a new type of serine/threonine kinase highly induced in the presence of serum and stimuli that produce synaptic plasticity (14, 15). SNK is one of the Plks that associate with cell cycle (16–18). The full-length

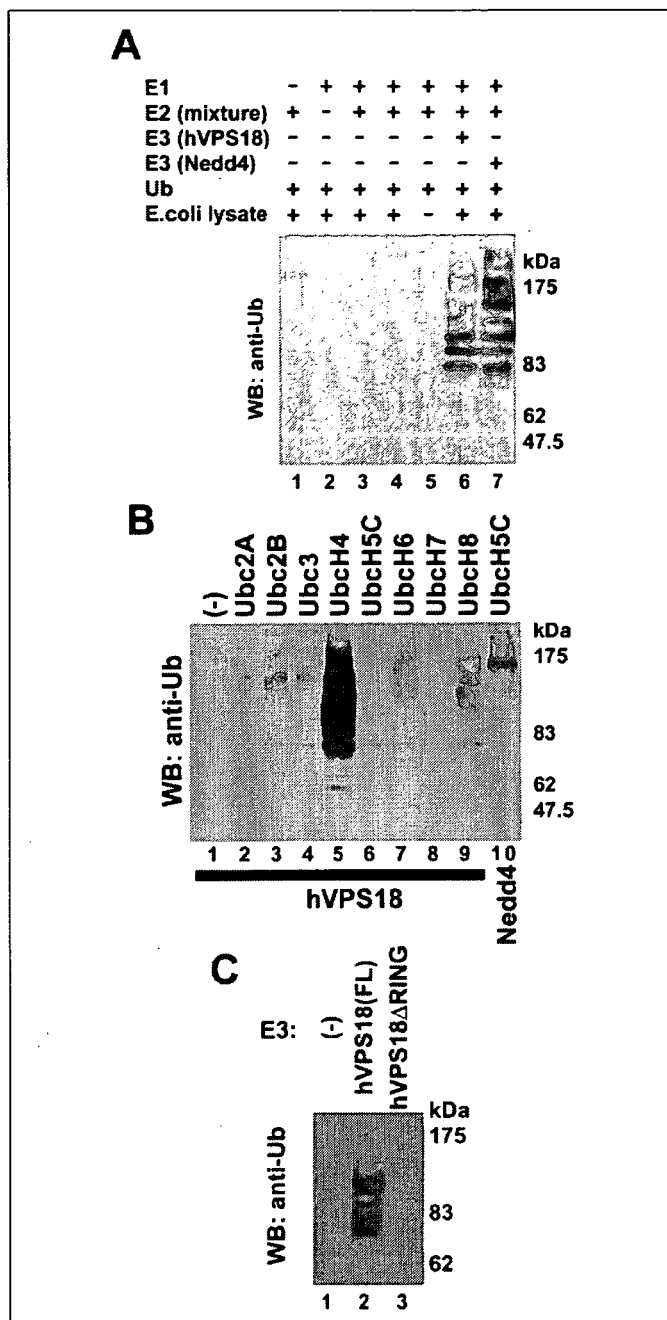


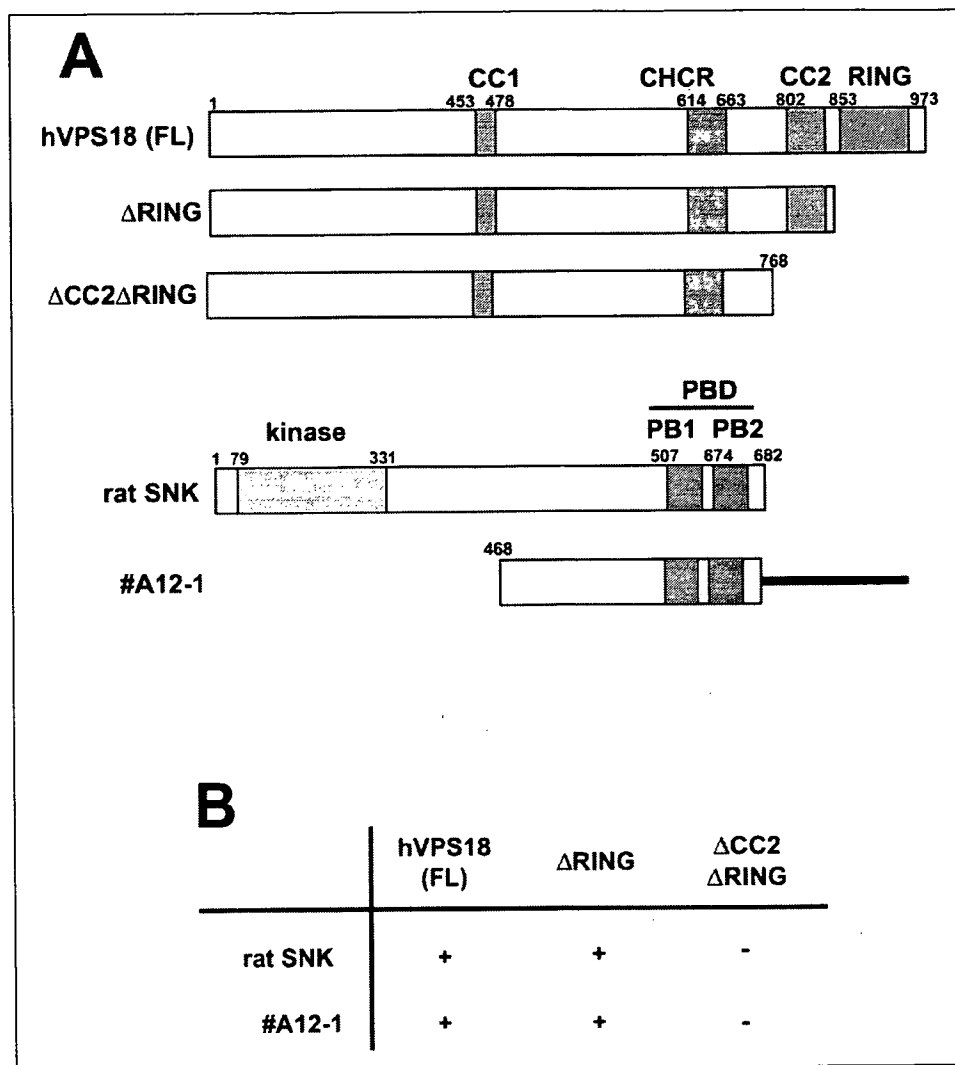
**FIGURE 1. hVPS18 is a RING-H2 type ubiquitin ligase.** A, the *in vitro* ubiquitylation reaction was performed in the presence or absence of purified His-hVPS18 or Nedd4, E1, E2-enzyme mixture, ubiquitin, and *E. coli* lysate as substrate at 25 °C for 30 min. After the reaction, the proteins were resolved by SDS-PAGE and detected by Western blot analyses using anti-ubiquitin antibody. The ubiquitylated proteins were detected in lanes 6 and 7. B, to examine E2 selectivity for hVPS18, the *in vitro* ubiquitylation reaction was performed. The ubiquitylation of proteins by hVPS18 was selectively mediated by UbcH4. C, the *in vitro* ubiquitylation reaction was performed in the presence of His-hVPS18 or His-hVPS18ΔRING. ΔRING, C-terminal deletion of RING-H2 of hVPS18. The RING-H2 domain is necessary for the ubiquitylation by hVPS18.

SNK cDNA revealed that SNK is a 682-amino acid protein with calculated molecular mass of 77.8 kDa, containing kinase domain at the N-terminal regions and polo-box domain (PBD) at the C-terminal regions (14, 19).

We further confirmed the interaction of hVPS18 and SNK using the two-hybrid assays. Results of β-galactosidase color reaction were summarized in Fig. 2B. The clone A12-1 and full-length SNK bind to both

## Ubiquitylation of SNK by hVPS18

**FIGURE 2. Interaction of hVPS18 and SNK in yeast cells.** *A*, schematic representation of hVPS18 (full-length,  $\Delta$ RING, and  $\Delta$ CC2 $\Delta$ RING), and SNK (full-length and #A12-1). The clone #A12-1 is a partial fragment of SNK isolated from the yeast two-hybrid screen.  $\Delta$ CC2, C-terminal deletion at the second coiled-coil region of hVPS18. *B*, the interaction of hVPS18 and SNK was confirmed by  $\beta$ -galactosidase assay in yeast cells. The interaction between hVPS18 and SNK was abolished when the second coiled-coil region of hVPS18 was deleted. +, detectable by  $\beta$ -galactosidase activity; -, not detectable. FL, full-length; CC, coiled-coil; CHCR, chattering heavy chain repeat; PBD, polo-box domain; PB, polo-box.



the full-length hVPS18 (FL) and hVPS18 lacking RING-H2 domain ( $\Delta$ RING), but not to hVPS18 lacking the C-terminal coiled-coil domain and RING-H2 domain ( $\Delta$ CC2 $\Delta$ RING). This suggests that hVPS18 interacts with SNK through the second coiled-coil domain.

**hVPS18 Interacts with SNK in Vitro and in Vivo**—To answer the question whether the full-length SNK interacts with hVPS18, we performed immunoprecipitation assays. HEK293T cells were transfected with Myc-SNK and HA-tagged hVPS11, hVPS18, hVPS16, and hVPS33a, respectively. As shown in Fig. 3A, SNK was efficiently co-immunoprecipitated with hVPS18 and the other Class C VPS. Please note that the interaction between SNK and hVPS18 is strongest among other members of Class C VPS complex. To further confirm the association of SNK and the Class C VPS *in vitro*, we performed an *in vitro* pull-down assay. The bacterial expressed GST-SNK was immobilized on glutathione beads, and insect-expressed His-tagged hVPS11, hVPS18, and hVPS16 were loaded. As shown in Fig. 3B (lanes 1–6), in a good agreement with the data obtained in the yeast two-hybrid screen, GST-SNK preferentially interact with His-hVPS18. As shown in Fig. 3B (lanes 7–12), hVPS11 and hVPS16 were retained with GST-SNK in the presence of hVPS18. These results suggest that the interaction between SNK and other Class C VPS in co-immunoprecipitation assay is partly mediated by hVPS18, and all of the Class C VPS proteins may constitute a large hetero-oligomeric complex *in vivo* (6).

Because the highly conserved PBD plays an important role for the correct subcellular localization and molecular interaction, we performed *in vitro* pull-down assays using the bacterially expressed GST proteins fuse to the various deletion forms of SNK. As shown in Fig. 4, SNK full-length and deletion mutants containing PBD at the C-terminal regions, efficiently bind to hVPS18, indicated that the PBD of SNK is involved in protein-protein interaction consistent with previous report (20, 21).

**VPS18 Ubiquitylates SNK in Vitro and in Vivo**—To answer the question whether SNK is ubiquitylated by hVPS18, we performed ubiquitylation assays of SNK *in vivo* and *in vitro*. COS7 cells were co-transfected with FLAG-tagged SNK, and various combinations of Myc-tagged hVPS18, hVPS11, and hVPS16, in the presence or absence of HA-tagged ubiquitin. As shown in Fig. 5A, SNK was heavily conjugated with HA-ubiquitin in the cells overexpressing hVPS18 (Fig. 5A, lane 3). The faint smearing in lanes 2, 4, and 5 suggests the possibility that SNK was ubiquitylated by endogenous VPS18 or other anonymous E3 of COS7 cells. It is necessary to observe the direct ubiquitylation of SNK by hVPS18 *in vitro*, we carried out ubiquitylation assays in which bacterially expressed GST-SNK proteins were incubated in the presence of E1, E2, His-hVPS18, ubiquitin, and ATP. As shown in Fig. 5B, SNK was ubiquitylated dependent on hVPS18, suggesting that SNK is one of the target substrates for hVPS18 E3 ubiquitin ligase.

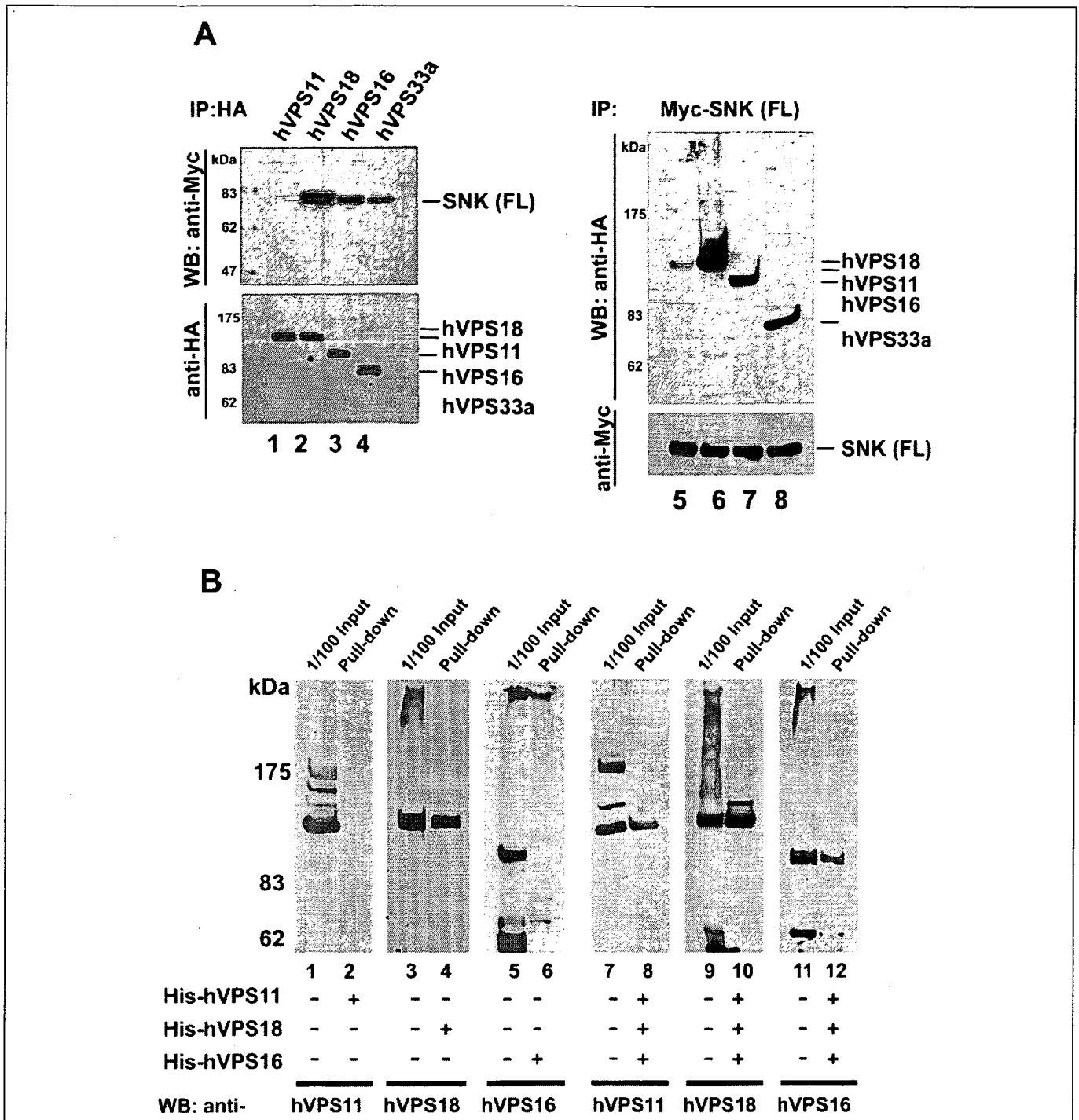


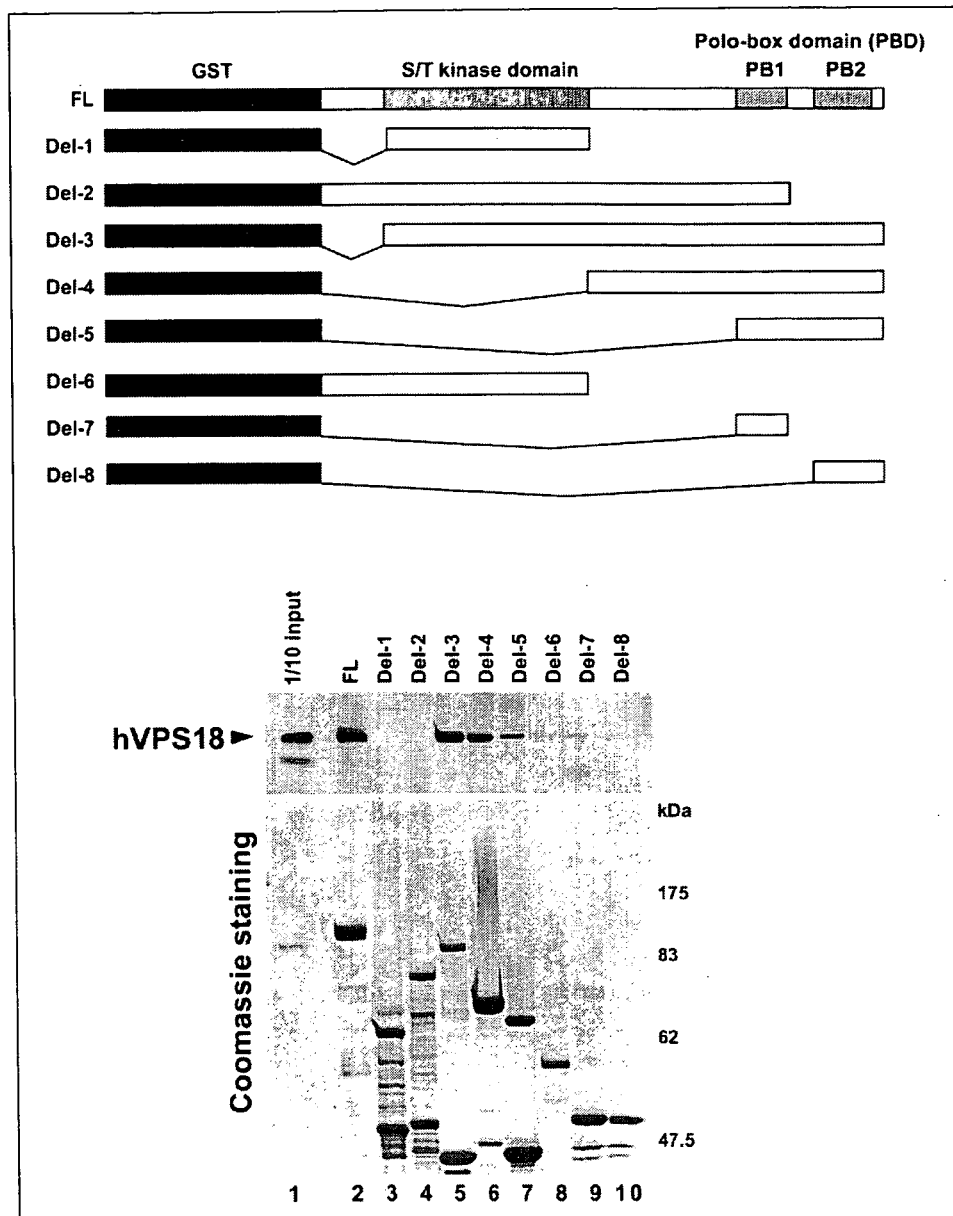
**FIGURE 3. Interaction of hVPS18 and SNK *in vivo* and *in vitro*.** *A* (left), HEK293T cells were co-transfected with Myc-SNK and either HA-tagged hVPS11, hVPS18, hVPS16, or hVPS33a, respectively. At 24 h post-transfection, whole cell lysates were immunoprecipitated using anti-HA antibody. Immunoprecipitates were resolved by SDS-PAGE and detected by Western blot analyses using anti-Myc antibody (upper panel). The membrane was then stripped and blotted with anti-HA antibody (lower panel). HA-hVPS18 strongly precipitated Myc-SNK (lane 2). Right, conversely, immunoprecipitation was performed using anti-Myc antibody, and the interacting molecules were detected by anti-HA antibody. *B*, GST-SNK was immobilized on glutathione-Sepharose 4B beads and incubated with His-tagged hVPS18, hVPS11, or/and hVPS16 at 25 °C for 30 min. The resin was washed and subjected to SDS-PAGE, and Western blot analyses were performed with indicated antibodies. His-hVPS18 interacted directly interacted with GST-SNK *in vitro*.

**HeLa Cell Lines That Overexpress hVPS18 or Knockdown hVPS18**—To characterize the physiological relation of SNK and hVPS18, we established HeLa cells that overexpress hVPS18 (HeLa-hVPS18(OE)) or shRNA interference of hVPS18 (HeLa-hVPS18(shRNA)) by lentivirus. After infection with the recombinant lentivirus, HeLa cells were treated with 10 μg/ml Blastidicin S, which is a selection antibiotic drug of the

recombinant lentivirus infection. After 7–14 days of incubation with Blastidicin S, the resistant colony was isolated and expanded. To confirm the expression level of hVPS18 and SNK, Western blot analyses were performed. Compared with the control HeLa cell, the cells treated with shRNA interference lentivirus of hVPS18 show up-regulated expression of SNK. Conversely, the cells overexpressing hVPS18 show

## Ubiquitylation of SNK by hVPS18

**FIGURE 4. Polo-box domain of SNK is necessary for binding with hVPS18 *in vitro*.** *Top*, schematic representation of SNK full-length and various deletion mutants used in the *in vitro* GST pull-down assays. *Bottom*, the *in vitro* pull-down assays of His-hVPS18 and either GST-SNK or various deletion mutants were performed. *Bottom*, GST-SNK proteins used in this study were shown as Coomassie Brilliant Blue (CBB) staining to confirm that the relatively equal amount of proteins was analyzed in each experiment.



down-regulated SNK (Fig. 6A). To define the subcellular localization of SNK and hVPS18, immunohistochemistry was performed using established HeLa cell lines as shown in Fig. 6B. Up-regulated expression of SNK was observed in the cells that knocked down hVPS18 by shRNA interference lentivirus, whereas down-regulated expression of SNK was observed in the cells overexpressing hVPS18. The reciprocal level of expression between hVPS18 and SNK strongly suggests the endogenous SNK expression is regulated, at least in part, by hVPS18.

To further analyze the role of hVPS18 in the SNK protein turnover, *in vivo* cell labeling by [<sup>35</sup>S]Met/[<sup>35</sup>S]Cys was performed. As shown in Fig. 7, the three lines of HeLa cells (control, hVPS18(OE), and hVPS18(shRNA)) were labeled and pulse-chased at five time points (0, 15, 30, 60, and 120 min). The total cell lysates were incubated with rat anti-SNK antibody, and the immunoreactive bands were resolved by SDS-PAGE. In general, polyubiquitylated proteins are promptly subjected to degradation by 26 S proteasome. In a good accordance with our results that SNK is ubiquitinated, the level of SNK protein degraded quickly (half-life, 20 min, Fig. 7B) as shown in the control

HeLa cells. When hVPS18 was overexpressed, the degradation of SNK protein was enhanced (half-life, 13.5 min, Fig. 7B). Conversely, the degradation of SNK protein was retarded in the HeLa cells knocked-down hVPS18 expression (half-life, 45 min, Fig. 7B). The degradation pattern was reproducible by using the independent antibody against SNK provided by Dr. M. Sheng (data not shown). These results suggest that the degradation of endogenous SNK in HeLa cells can be regulated by the level of hVPS18 expression.

*Delayed Entry to S Phase When Overexpressed with hVPS18*—Our hypothesis is that hVPS18 is involved in the degradation of SNK. It was previously reported that the kinase activity of SNK is required for centriole duplication close to the G<sub>1</sub> to S phase transition (16). Cultured SNK<sup>-/-</sup> embryonic fibroblasts showed delayed entry to S phase (18). We thus examined the cell-cycle progression of HeLa cells overexpressing hVPS18. Although the profile of cell cycle between control HeLa cells and hVPS18 overexpressing HeLa cells was almost similar, the proportion of cells to S phase after 20 h was significantly lower than the control HeLa cells (Fig. 8). These results are in good accordance with the